

Beauty-charm meson family with coupled channel effects and their strong decays*

Wei Hao (郝伟)^{1†} Ruilin Zhu (朱瑞林)^{2,3‡}

¹School of Physics, Nankai University, Tianjin 300071, China

²Department of Physics and Institute of Theoretical Physics, Nanjing Normal University, Nanjing, Jiangsu 210023, China

³Peng Huanwu Innovation Research Center, Institute of Theoretical Physics, Chinese Academy of Sciences, Beijing 100190, China

Abstract: We systematically examined the mass spectra and their two-body hadronic decays of the beauty-charm meson family considering coupled channel effects. Our results can effectively explain the observed B_c meson spectrum, and the prediction of the mass spectrum for unobserved beauty-charm mesons can be tested in future experiments. Compared with previous studies, we systematically examine the beauty-charm meson family within the coupled channel components. The $1S$ state in beauty-charm meson family has few percent of coupled channel component, while the $2S$, $1P$, and $1D$ states have more than ten percent of coupled channel component. The two-body hadronic decay widths of the 2^3P_2 state is as narrow as 3 MeV. The two-body hadronic decay widths of 3^1S_0 , 3^3S_1 , 2^3D_1 , $2D$, $2D'$, and 2^3D_3 are approximately 109, 67, 60, 57, 201, and 76 MeV, respectively. Furthermore, the mixing effects between $B_c(n^3L_L)$ and $B_c(n^1L_L)$ states are discussed.

Keywords: beauty-charm meson, coupled channel effects, strong decays

DOI: 10.1088/1674-1137/ad75f5

I. INTRODUCTION

The understanding of hadron structures and their transitions at Fermi scale is a fundamental issue from both the theoretical and experimental aspects in particle physics. Given the meson spectrum, the beauty-charm meson family is relatively incomplete when compared with other systems. To date, only three beauty-charm mesons have been observed in experiments, i.e., the $B_c(1S)$, $B_c(2S)$ and $B_c^*(2S)$ [1].

The ground state $B_c(1^1S_0)$ of beauty-charm family was first discovered in 1998 by CDF at Fermilab [2]. The latest average mass for this state is determined as $6274.47 \pm 0.27 \pm 0.17$ MeV [1]. A new structure was first discovered in $B_c^+\pi^+\pi^-$ invariant mass spectrum with subprocess $B_c^+ \rightarrow J/\psi\pi^+$ using the sample corresponding to 4.9 fb^{-1} of 7 TeV and 19.2 fb^{-1} of 8 TeV pp collision data acquired by the ATLAS experiment at the LHC in 2014 [3]. Then, two radially excited beauty-charm states $B_c(2^1S_0)$ and $B_c^*(2^3S_1)$ as opposed to one peak are dis-

covered in $B_c^+\pi^+\pi^-$ invariant mass spectrum in the same channels from both the CMS and LHCb experiments [4, 5]. The combined average mass for $B_c(2^1S_0)$ is determined as 6871.2 ± 0.1 MeV [1]. For the vector excited state, $B_c^*(2^3S_1)$ first decays via hadronic transition $B_c^{*+}(2^3S_1) \rightarrow B_c^{*+}(1^3S_1)\pi^+\pi^-$ and then vector $B_c^{*+}(1^3S_1)$ decays via electromagnetic transition $B_c^{*+}(1^3S_1) \rightarrow B_c^+(1^1S_0) + \gamma$. However, the radiated photon is soft with energy of approximately 60 MeV, which is not reconstructed among ATLAS, CMS, and LHCb experiments. Thus, the determination of the mass of $B_c^{*+}(2^3S_1)$ relies on the precise information of $B_c^{*+}(1^3S_1)$. Additionally, other beauty-charm meson states, including orbitally excited states, have not been observed in experiments to date. This requires precise theoretical predictions.

In theoretical aspects, the mass spectra of beauty-charm mesons have been examined in many studies. For example, quark potential models [6–15], QCD sum rule [16–20], heavy quark effective theory [21], and Dyson-Schwinger equation approach of QCD [22, 23]. Further-

Received 3 June 2024; Accepted 2 September 2024; Published online 3 September 2024

* Supported by the National Natural Science Foundation of China (12322503, 12047503, 12075124), and the Natural Science Foundation of Jiangsu Province, China (BK20211267)

† E-mail: haowei@nankai.edu.cn

‡ E-mail: rlzhu@njnu.edu.cn(Corresponding author)

 Content from this work may be used under the terms of the Creative Commons Attribution 3.0 licence. Any further distribution of this work must maintain attribution to the author(s) and the title of the work, journal citation and DOI. Article funded by SCOAP³ and published under licence by Chinese Physical Society and the Institute of High Energy Physics of the Chinese Academy of Sciences and the Institute of Modern Physics of the Chinese Academy of Sciences and IOP Publishing Ltd

more, the properties of low-lying B_c mesons are also investigated in lattice QCD based on the first principles [24–26].

Up to now, the Godfrey-Isgur quenched approach in quark potential models [14] is usually considered to provide a good and systematical description for most of the meson spectra. However, the quenched quark models sometimes poorly explain higher excited states beyond the two-body threshold because they miss the generation of the light quark-antiquark pairs which enlarge the Fock space of the initial state [27]. These multiquark components will change the Hamiltonian of the conventional quark potential models and then lead to mass shift and mixing among states with the same quantum numbers. If the initial state exceeds two-body threshold, then the open channel strong decay will be allowed. This implies that the unquenched quark model includes virtual hadronic loops. The hadronic loop has turned out to be highly non-trivial and can lead to mass shifts to the bare hadron states and contribute continuum components to the physical hadron states [28].

The coupled-channel model as one of the unquenched quark model, which is usually neglected, will manifest as a coupling to meson-meson (meson-baryon) channels and lead to mass shifts. These effects are introduced explicitly into the constituent quark model via a QCD-inspired 3P_0 pair-creation mechanism. The pair-creation mechanism is inserted at the quark level and one-loop diagrams are calculated by summing over the possible intermediate states [29]. It has been shown that the coupled-channel effects play an important role for describing the mesons spectra, such as charmonium [30–33], bottomonium [27–29, 34], and charmed-strange mesons [35–46].

In this study, we will use this type of unquenched quark model to examine the beauty-charm mesons. We will systematically investigate the mass spectrum of the beauty-charm mesons within the nonrelativistic quark model by considering the mass shifts from the coupled-channel effects. Additionally, the two-body hadronic decays are also examined. The paper is arranged as follows. The theoretical formalism in coupled channel framework is provided in Section II, where the nonrelativistic quenched quark model and 3P_0 model are introduced. The beauty-charm meson spectrum, including coupled channel effects, molecule and two quark components, and two body hadronic decay widths, are provided in Section III. Finally, we provide the summary in Section IV.

II. THEORETICAL FORMALISM

A. Quenched quark model

First, we introduce a nonrelativistic quark model to denote the quenched quark interactions. Furthermore,

Hamiltonian H_Q can be expressed as:

$$H_Q = m_b + m_{\bar{c}} + \frac{\nabla^2}{2m_r} - C_F \frac{\alpha_s}{r} + br + C_{b\bar{c}} \\ + \frac{32\alpha_s\sigma^3 e^{-\sigma^2 r^2}}{9\sqrt{\pi}m_b m_{\bar{c}}} \mathbf{S}_b \cdot \mathbf{S}_{\bar{c}} + H_{SL}, \quad (1)$$

where the reduced quark mass m_r satisfies $m_r = m_b m_{\bar{c}} / (m_b + m_{\bar{c}})$. Specifically, \mathbf{S}_i denotes the heavy quark spin operator. The linear confining assumption is employed and parameters m_b , $m_c = m_{\bar{c}}$, $C_{b\bar{c}}$, σ , b , and α_s in the quenched quark model Hamiltonian will be refitted from the knowledge of the existing hadrons.

The left spin and orbital related term H_{SL} has the expression:

$$H_{SL} = \left(\frac{\mathbf{S}_b}{2m_b^2} + \frac{\mathbf{S}_{\bar{c}}}{2m_{\bar{c}}^2} \right) \cdot \mathbf{L} \left(\frac{1}{r} \frac{dV_c}{dr} + \frac{2}{r} \frac{dV_1}{dr} \right) \\ + \frac{\mathbf{S}_+ \cdot \mathbf{L}}{m_b m_{\bar{c}}} \left(\frac{1}{r} \frac{dV_2}{dr} \right) + \frac{3\mathbf{S}_b \cdot \hat{\mathbf{r}} \mathbf{S}_{\bar{c}} \cdot \hat{\mathbf{r}} - \mathbf{S}_b \cdot \mathbf{S}_{\bar{c}}}{3m_b m_{\bar{c}}} V_3 \\ + \left[\left(\frac{\mathbf{S}_b}{m_b^2} - \frac{\mathbf{S}_{\bar{c}}}{m_{\bar{c}}^2} \right) \cdot \mathbf{L} + \frac{\mathbf{S}_-}{m_b m_{\bar{c}}} \cdot \mathbf{L} \right] V_4, \quad (2)$$

where \mathbf{L} denotes the orbital angular momentum between beauty charm quarks. $\mathbf{S}_\pm = \mathbf{S}_b \pm \mathbf{S}_{\bar{c}}$. The expressions for each potential are as follows:

$$V_c = -C_F \frac{\alpha_s}{r} + br, \\ V_1 = -br - \frac{2}{9\pi} \frac{\alpha_s^2}{r} [9\ln(\sqrt{m_b m_{\bar{c}}} r) + 9\gamma_E - 4], \\ V_2 = -C_F \frac{\alpha_s}{r} - \frac{1}{9\pi} \frac{\alpha_s^2}{r} [-18\ln(\sqrt{m_b m_{\bar{c}}} r) + 54\ln(\mu r) \\ + 36\gamma_E + 29], \\ V_3 = -\frac{4\alpha_s}{r^3} - \frac{1}{3\pi} \frac{\alpha_s^2}{r^3} [-36\ln(\sqrt{m_b m_{\bar{c}}} r) + 54\ln(\mu r) \\ + 18\gamma_E + 31], \\ V_4 = \frac{1}{\pi} \frac{\alpha_s^2}{r^3} \ln\left(\frac{m_{\bar{c}}}{m_b}\right), \quad (3)$$

where γ_E denotes Euler constant. Furthermore, $SU(3)$ color factors are $C_F = 4/3$ and $C_A = 3$. The renormalization scale $\mu = 1$ GeV is adopted as in Refs. [47–52].

The spin operator $\mathbf{S}_- = \mathbf{S}_b - \mathbf{S}_{\bar{c}}$ can lead to the mixing of the beauty-charm mesons with identical total angular momentum but with different total spins. For example, mixing between $B_c(n^3 L_L)$ and $B_c(n^1 L_L)$ states occurs, and this can be described by mixing matrix by introducing a mixing angle θ_{nL} [14, 53] as follows:

$$\begin{pmatrix} B_{cL}(nL) \\ B'_{cL}(nL) \end{pmatrix} = \begin{pmatrix} \cos\theta_{nL} & \sin\theta_{nL} \\ -\sin\theta_{nL} & \cos\theta_{nL} \end{pmatrix} \begin{pmatrix} B_c(n^1 L_L) \\ B_c(n^3 L_L) \end{pmatrix}, \quad (4)$$

where the physical observed states are denoted as $B_{cL}(nL)$ and $B'_{cL}(nL)$.

The mixing angle is determined by the spin-orbit term H_{SL} . The term include two parts, symmetric part H_{sym} and antisymmetric part H_{anti} . These two parts can be expressed as [48]:

$$H_{\text{sym}} = \frac{\mathbf{S}_+ \cdot \mathbf{L}}{2} \left[\left(\frac{1}{2m_q^2} + \frac{1}{2m_{\bar{q}}^2} \right) \left(\frac{1}{r} \frac{dV_c}{dr} + \frac{2}{r} \frac{dV_1}{dr} \right) + \frac{2}{m_q m_{\bar{q}}} \left(\frac{1}{r} \frac{dV_2}{dr} \right) + \left(\frac{1}{m_q^2} - \frac{1}{m_{\bar{q}}^2} \right) V_4 \right], \quad (5)$$

$$H_{\text{anti}} = \frac{\mathbf{S}_- \cdot \mathbf{L}}{2} \left[\left(\frac{1}{2m_q^2} - \frac{1}{2m_{\bar{q}}^2} \right) \left(\frac{1}{r} \frac{dV_c}{dr} + \frac{2}{r} \frac{dV_1}{dr} \right) + \left(\frac{1}{m_q^2} + \frac{1}{m_{\bar{q}}^2} + \frac{2}{m_q m_{\bar{q}}} \right) V_4 \right]. \quad (6)$$

When the heavy-light mesons have different total spins but with same total angular momentum, the spin-orbit mixing will occur. The mixing angle can be estimated by the antisymmetric part H_{anti} . Furthermore, H_{anti} provides the influence of non-diagonal terms, and the mixed angle can be extracted via diagonalization,

B. Gaussian expansion method

The Gaussian expansion method is a high-precision method for solving Schrodinger equation. The method was proposed by E. Hiyama [54]. By using Gaussian basis functions, it can describe accurately short-range correlations and long-range asymptotic behavior and highly oscillatory character of wave functions in bound and scattering states of the systems. The method is widely used to calculate hadron spectrum [27, 55, 56]. For a given two-body Schrodinger equation:

$$\left[-\frac{\hbar^2}{2\mu} \nabla^2 + V(r) - E \right] \psi_{lm}(\mathbf{r}) = 0, \quad (7)$$

where μ denotes the reduced mass and $V(r)$ denotes a central potential. The equation can be solved by wave function $\psi_{lm}(\mathbf{r})$ in terms of a set of Gaussian basis functions, $\phi_{nlm}^G(\mathbf{r}) = \phi_{nl}^G(r) Y_{lm}(\hat{\mathbf{r}})$. Furthermore, the functions can be expressed as follows:

$$\psi_{lm}(\mathbf{r}) = \sum_{n=1}^{n_{\max}} c_{nl} \phi_{nlm}^G(\mathbf{r}), \quad (8)$$

$$\phi_{nlm}^G(\mathbf{r}) = \phi_{nl}^G(r) Y_{lm}(\hat{\mathbf{r}}), \quad (9)$$

$$\phi_{nl}^G(r) = N_{nl} r^l e^{-\nu_n r^2}, \quad (10)$$

$$N_{nl} = \left(\frac{2^{l+2} (2\nu_n)^{l+\frac{3}{2}}}{\sqrt{\pi} (2l+1)!!} \right)^{1/2}, \quad (n = 1 - n_{\max}). \quad (11)$$

The constant N_{nl} is normalization constant, which can be determined by $\langle \phi_{nlm}^G | \phi_{nlm}^G \rangle = 1$. Hence, set $\{\phi_{nlm}^G; n = 1 - n_{\max}\}$ is a non-orthogonal set.

C. Coupled channel framework

The quenched quark potential model only includes the interaction between heavy quark pair. However, the hadronic loop interaction can also play a role via the generation of the light quark pair in $b\bar{c} \rightarrow (b\bar{q})(q\bar{c})$. Furthermore, the hadronic loop interaction becomes more important for the higher excited beauty-charm mesons. The coupled channel framework provides a good description for the hadronic loop interactions.

In this framework, the beauty-charm meson state can be expressed as:

$$|\psi\rangle = \begin{pmatrix} c_0 |\psi_0\rangle \\ \sum_{BD} \int d^3 p c_{BD}(p) |BD; p\rangle \end{pmatrix}, \quad (12)$$

where c_0 denotes the $b\bar{c}$ bare state probability amplitude, while $c_{BD}(p)$ denotes the beauty meson B and charm meson D molecular component probability amplitude with relative momentum p . To normalize the state, we impose the condition $|c_0|^2 + \sum_{BD} \int d^3 p |c_{BD}(p)|^2 = 1$.

The total Hamiltonian in coupled channel framework can be expressed as:

$$H = \begin{pmatrix} H_Q & H_I \\ H_I & H_{BD} \end{pmatrix}, \quad (13)$$

where H_{BD} denotes the Hamiltonian for beauty meson B and charm meson D system as:

$$H_{BD} = E_{BD} = \sqrt{m_B^2 + p^2} + \sqrt{m_D^2 + p^2}. \quad (14)$$

H_I leads to coupling between $b\bar{c}$ bare state and BD molecule component. In the following, the 3P_0 model, where the generated light quark pairs have identical quantum numbers $J^{PC} = 0^{++}$ in vacuum, is employed to analyze the mixing of $b\bar{c}$ bare state and BD molecule component [64–66].

Then, we solve the spectrum eigen equation as fol-

lows:

$$H|\psi\rangle = M|\psi\rangle, \quad (15)$$

where M denotes the final mass for the beauty-charm mesons in coupled channel framework. Practically, the eigenvalue M can be rewritten as [29, 30, 32, 34]:

$$M = M_Q + \Delta M, \quad (16)$$

$$\Delta M = \sum_{BD} \int_0^\infty p^2 dp \frac{|\langle BD; p | T^\dagger | \psi_0 \rangle|^2}{M - E_{BD}}, \quad (17)$$

where M_Q denotes the eigenvalue for the quenched Hamiltonian H_Q , while ΔM denotes the mass shift from the coupled channel effect. Operator T^\dagger in 3P_0 model can be expressed as [29, 32, 34]:

$$T^\dagger = -3\gamma_0^{\text{eff}} \int d\vec{p}_1 d\vec{p}_2 \delta(\vec{p}_1 + \vec{p}_2) C_{12} F_{12} e^{-r_q^2(\vec{p}_1 - \vec{p}_2)^2/6} [\chi_{12} \times \mathcal{Y}_1(\vec{p}_1 - \vec{p}_2)]_0^{(0)} b_1^\dagger(\vec{p}_1) d_2^\dagger(\vec{p}_2), \quad (18)$$

where operators $b_1^\dagger(\vec{p}_1)$ and $d_2^\dagger(\vec{p}_2)$ create a light quark pair. The light quark pair creation strength is denoted as $\gamma_0^{\text{eff}} = \frac{m_u}{m_i} \gamma_0$ with $\gamma_0 = 0.4$ and $i = u, d, s$ [7]. The color, flavor, and spin wave functions for the light quark pair are C_{34} , F_{34} , and χ_{34} , respectively. Furthermore, r_q denotes a width parameter of Gaussian factor, whose value is determined by analyzing meson decays. The Gaussian factor reflects the effective scale of quark pairs via smearing. This parameter is an improvement of 3P_0 model. It is physically motivated and necessary to obtain a finite result when one sums over a complete set of virtual decay channels [67]. The value of r_q is in the range of 0.25 to 0.35 fm [67–70]. We use the value $r_q = 0.3$ fm in the following calculation.

To weigh the importance of coupled channel effects, it is useful to investigate the probabilities of $b\bar{c}$ bare component and BD molecule component in the physical state. The probability of quenched $b\bar{c}$ bare component can be expressed as:

$$P_{b\bar{c}} \equiv |c_0|^2 = \left(1 + \sum_{BD} \int_0^\infty p^2 dp \frac{|\langle BD; p | T^\dagger | \psi_0 \rangle|^2}{(M - E_{BD})^2} \right)^{-1}. \quad (19)$$

Then, the probability of BD molecule component can be naturally expressed as $P_{\text{molecule}} = \sum_{BD} P_{BD} = 1 - P_{b\bar{c}}$. Given that bare state mass is above the BD threshold, it is not

possible to normalize the wave functions. Hence, we cannot estimate the proportion of the channel.

For highly excited beauty-charm mesons above the BD threshold, they undergo direct two-body decay into a beauty meson and charm meson. The strong decay width is related to the imaginary part in ΔM and can be expressed as:

$$\Gamma_{BD} = 2\pi p_0 \frac{E_B(p_0)E_D(p_0)}{M} |\langle BD; p_0 | T^\dagger | \psi_0 \rangle|^2. \quad (20)$$

III. RESULTS AND DISCUSSIONS

Given that only B_c mesons have experimental information, it is difficult to fit all parameters. Hence, we adopt a strategy similar to that in Ref. [7]. Although there are no experimental data for $B_c^*(1^3S_1)$ and $B_c^*(2^3S_1)$ masses, their values can be estimated as approximately 6334 and 6900 MeV, respectively. Furthermore, given that the hyperfine mass splitting in bottomonium family is measured as $\Delta M_{b\bar{b}(1S)} = 62.3 \pm 3.2$ MeV and $\Delta M_{b\bar{b}(2S)} = 24 \pm 4$ MeV [1], the hyperfine mass splitting in beauty-charm meson family is considered as small as $m_{B_c^*} - m_{B_c} \geq \Delta M_{b\bar{b}(1S)} = 62.3 \pm 3.2$ MeV and $m_{B_c^*(2S)} - m_{B_c(2S)} \geq \Delta M_{b\bar{b}(2S)} = 24 \pm 4$ MeV because the hyperfine mass splitting is inversely proportional to the heavy quark mass. Based on experimental results and theoretical discussions, we have four data points $B_c(1^1S_0)$, $B_c^*(1^3S_1)$, $B_c(2^1S_0)$, and $B_c^*(2^3S_1)$ with masses 6274, 6334, 6871, and 6900 MeV, respectively. We use these values to fit the model parameters α_s , b , σ . For the other parameters in the model, we use commonly used values, which can describe other mesons well [7, 47, 49]. It should be noted that we do not fit all parameters in the model due to the lack of sufficient experimental data for fitting. The final refitted parameters are listed in Table 1.

With the parameters in Table 1, the mass spectrum and mass shifts of the B_c mesons can be estimated. The

Table 1. Parameters refitted in this study.

Parameter	This work
m_n	0.45 GeV
m_s	0.55 GeV
m_c	1.43 GeV
m_b	4.5 GeV
α_s	0.51851
b	0.16178 GeV ²
σ	1.3424 GeV
$C_{b\bar{c}}$	0.454 GeV
γ_0	0.4

Table 2. Beauty charm meson family spectrum (in MeV). The third column denotes the naive mass in quenched quark model; the fourth column denotes the mass shift from coupled channel effects; the fifth column denotes the final results for the beauty charm meson family spectrum; the last column is the latest experimental data [1]. For comparison, other theoretical predictions from quenched quark models are also listed. The mixing angles of $1P$, $2P$, $1D$, and $2D$ are determined as -35.0° , -36.3° , -42.8° and -43.9° , respectively.

$n^{2S+1}L_J$	State	M_0	ΔM	M	EPI [57]	EMK [58]	MAS [59]	RR [60]	QL [7]	GI [61]	XJL [12]	DE [62]	APM [10]	RPP [1]
1^1S_0	B_c^+	6337	-65	6272	6274	6277	6277	6277	6271	6271	6271	6270	6275	6274.47 ± 0.32
1^3S_1	-	6405	-70	6335	-	-	-	-	6326	6338	6338	6332	6314	$6331 \pm 4 \pm 6^a$
2^1S_0	$B_c(2S)^\pm$	6989	-114	6874	6845	7038	7383	6814	6871	6855	6855	6835	6838	6871.2 ± 1.0
2^3S_1	-	7013	-116	6897	-	-	-	-	6890	6887	6886	6881	6850	-
3^1S_0	-	7393	-141	7252	7124	7798	7206	7351	7239	7250	7220	7193	-	-
3^3S_1	-	7410	-129	7281	-	-	-	-	7252	7272	7240	7235	-	-
1^3P_0	-	6803	-98	6706	6519	7799	7042	6340	6714	6706	6701	6699	6672	-
$1P$	-	6852	-102	6750	-	-	-	-	6757	6741	6745	6734	6766	-
$1P'$	-	6887	-102	6785	-	-	-	-	6776	6750	6754	6749	6828	-
1^3P_2	-	6906	-104	6802	-	-	-	-	6787	6768	6773	6762	6776	-
2^3P_0	-	7226	-127	7099	6959	-	6663	6851	7107	7122	7097	7091	6914	-
$2P$	-	7264	-136	7128	-	-	-	-	7134	7145	7125	7126	7259	-
$2P'$	-	7300	-135	7165	-	-	-	-	7150	7150	7133	7145	7322	-
2^3P_2	-	7316	-144	7172	-	-	-	-	7160	7164	7148	7156	7232	-
1^3D_1	-	7147	-124	7023	6813	-	-	-	7020	7041	7023	7072	7078	-
$1D$	-	7154	-121	7033	-	-	-	-	7024	7028	7032	7077	7009	-
$1D'$	-	7163	-122	7041	-	-	-	-	7032	7036	7039	7079	7154	-
1^3D_3	-	7163	-120	7043	-	-	-	-	7030	7045	7042	7081	6980	-
2^3D_1	-	7496	-136	7360	-	-	-	-	7336	-	7327	-	-	-
$2D$	-	7505	-150	7355	-	-	-	-	7343	-	7335	-	-	-
$2D'$	-	7509	-130	7380	-	-	-	-	7347	-	7340	-	-	-
2^3D_3	-	7514	-175	7338	-	-	-	-	7348	-	7344	-	-	-

^aThis result is from Lattice QCD simulation [63]. Combing LHCb data and Lattice QCD result, the mass of $B_c^*(2^3S_1)$ is determined as 6897 ± 12 MeV.

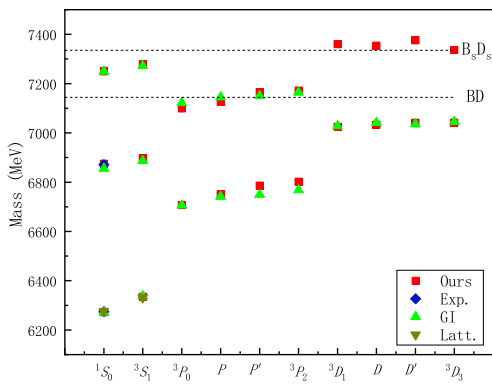


Fig. 1. (color online) Beauty-charm meson family spectrum. "Exp." denotes the current experimental values from the latest PDG [1] and our quenched quark model results are depicted as "Ours". The unquenched quark model results from Ref. [14] are shown as "GI". The Lattice results from Ref. [63] are shown as "Latt.". The dashed lines denote the threshold positions of BD and $B_s D_s$, respectively.

results are shown in Fig. 1, with numbers listed in Table 2 and Table 3. The mixing angles of $1P$, $2P$, $1D$, and $2D$ states can be also calculated, which are -35.0° , -36.3° , -42.8° and -43.9° , respectively. The mixing angles are close to B mesons $\theta_{1P} = -34.6^\circ$, $\theta_{2P} = -36.1^\circ$, $\theta_{1D} = -39.6^\circ$, $\theta_{2D} = -39.7^\circ$ and B_s mesons $\theta_{1P} = -34.9^\circ$, $\theta_{2P} = -36.1^\circ$, $\theta_{1D} = -39.8^\circ$, and $\theta_{2D} = -39.8^\circ$ [48].

The spectra of B_c mesons have been examined in many studies [7, 10, 12, 57–62, 71]. We listed their results in Table 2. It can be observed that different theoretical models predict the mass of $B_c^+(1^1S_0)$ in accordance with experimental results. For state $B_c(2S)^\pm$, the predicted mass corresponds to 6845 MeV via exact quantization rule approach [57], 6814 MeV via asymptotic iteration method [60], 6871 MeV via nonrelativistic quark model [7], and 6855 MeV via relativistic quark model [61]. These values are consistent with experimental data value of 6871.2 ± 1.0 MeV. However, the given mass val-

ues of 7038 MeV via analytical exact iteration method [58], 7383 MeV via non-relativistic quark model using Nikiforov-Uvarov method [59], and 6814 MeV via asymptotic iteration method [60] deviate significantly from the experimental results. These theoretical studies have enriched our understanding of the properties of B_c mesons. However, due to the limited experimental information on B_c mesons, there are still significant differences in the theoretical research results. Further experimental data is required to enhance and optimize theoretical understanding.

We predicted that the masses of $B_c(1^1S_0)$ and $B_c(2^1S_0)$ are 6272 and 6874 MeV, respectively, which are close to the experimental values of 6274.47 ± 0.32 MeV and 6871.2 ± 1.0 MeV. Furthermore, we show the theoretical results of the other states in beauty-charm meson family. We expect that more experimental information can be found to support our results.

For states below BD threshold, the probabilities of each coupled channel can be estimated. The probabilities are listed in [Table 4](#). Hence, all the states have coupled channel components. Specifically, when comparing $1S$, $2S$, $1P$, and the $1D$ states, the $2P$ states have larger non-

$b\bar{c}$ components. For $1S$ -wave states, we predicted they have 96% $b\bar{c}$ components. This implies that the coupled channel components is just 4%. For other states, we predicted $b\bar{c}$ component probabilities for $2S$, $1P$, $2P$, and $1D$ states, which are approximately 86%, 90%, 67%, and 84%, respectively.

For states, which have large masses, the strong decay channels will be open, and strong decay widths are shown in [Table 5](#). For $1S$ -wave, $2S$ -wave, and $1P$ -wave, most of $2P$ -wave and $1D$ -wave states, their masses are below the BD threshold and cannot undergo strong decay into BD states. Hence, we just discuss the strong decay of the $B_c(2^3P_2)$, $3S$ -wave, and $2D$ -wave B_c mesons. For $B_c(2^3P_2)$, it can just decay to BD final states with decay width of approximately 3 MeV. For $3S$ -wave states, $B_c(3^1S_0)$ can strong decay to B^*D with predicted width of 109 MeV, while the $B_c(3^3S_1)$ can strong decay to BD and B^*D with predicted width 10 and 57 MeV, whose total decay width becomes 67 MeV. For the $2D$ -wave states, the total decay widths of the $B_c(2^3D_1)$, $B_c(2D)$, $B_c(2D')$, and 2^3D_3 states are 60, 57, 201, and 76 MeV, respectively. The $B_c(2^3D_1)$ dominantly decay into BD^* and B^*D^* with predicted widths of 28 and 22 MeV. The $B_c(2D)$ can

Table 3. Mass shift ΔM (in MeV) for beauty charm mesons from different channels.

State	BD	BD^*	B^*D	B^*D^*	$B_s D_s$	$B_s D_s^*$	$B_s^* D_s$	$B_s^* D_s^*$	Total
1^1S_0	0	-13	-11	-25	0	-4	-4	-9	-65
1^3S_1	-4	-9	-8	-31	-1	-3	-3	-11	-70
2^1S_0	0	-23	-23	-44	0	-6	-6	-12	-114
2^3S_1	-8	-15	-16	-52	-2	-4	-4	-14	-116
3^1S_0	0	-36	-23	-60	0	-6	-6	-11	-142
3^3S_1	3	-32	1	-79	-2	-4	-4	-13	-130
1^3P_0	-12	0	0	-63	-3	0	0	-20	-98
$1P$	0	-20	-19	-39	0	-6	-6	-12	-102
$1P'$	0	-16	-15	-47	0	-5	-4	-15	-102
1^3P_2	-10	-15	-14	-42	-3	-5	-4	-13	-104
2^3P_0	-33	0	0	-72	-4	0	0	-18	-127
$2P$	0	-27	-34	-51	0	-6	-6	-12	-136
$2P'$	0	-24	-33	-54	0	-5	-5	-13	-135
2^3P_2	-19	-18	-21	-61	-3	-4	-4	-13	-143
1^3D_1	-13	-5	-6	-75	-3	-1	-1	-21	-124
$1D$	0	-24	-25	-47	0	-6	-6	-13	-121
$1D'$	0	-21	-22	-54	0	-5	-5	-15	-122
1^3D_3	-13	-18	-17	-47	-3	-5	-4	-12	-120
2^3D_1	-7	0	1	-104	-6	-1	-2	-17	-136
$2D$	0	-28	-17	-83	0	-6	-6	-11	-150
$2D'$	0	-13	-12	-79	0	-5	-7	-12	-130
2^3D_3	-10	-23	-20	-102	-3	-4	-4	-11	-175

Table 4. Two quark and molecule probabilities (in %) in the coupled channels framework.

State	BD	BD^*	B^*D	B^*D^*	$B_s D_s$	$B_s D_s^*$	$B_s^* D_s$	$B_s^* D_s^*$	P_{molecule}	$P_{b\bar{c}}$
1^1S_0	0	0.7	0.8	1.4	0	0.2	0.2	0.4	3.7	96.3
1^3S_1	0.3	0.5	0.6	1.8	0.1	0.1	0.2	0.5	4.3	95.7
2^1S_0	0	2.8	3.9	5.1	0	0.5	0.7	1.1	14.0	86.0
2^3S_1	1.6	1.9	2.7	6.2	0.2	0.4	0.5	1.3	14.8	85.2
1^3P_0	1.8	0	0	5.1	0.4	0	0	1.3	8.6	91.4
1^1P_1	0	1.8	2.4	3.5	0	0.4	0.5	0.9	9.6	90.4
1^3P_1	0	1.6	2.1	4.0	0	0.4	0.4	1.0	9.5	90.5
1^3P_2	1.2	1.3	1.7	4.1	0.3	0.3	0.4	1.0	10.2	89.8
2^3P_0	22.5	0	0	9.0	0.7	0	0	1.4	33.7	66.3
2^1P_1	0	5.3	16.7	8.4	0	0.6	0.8	1.1	32.9	67.1
2^3P_1	0	5.3	18.3	7.5	0	0.5	0.7	1.1	33.4	66.6
1^3D_1	4.3	0.9	1.5	8.0	0.4	0.1	0.2	1.7	17.1	82.9
1^1D_2	0	3.2	4.7	5.8	0	0.6	0.7	1.1	16.2	83.8
1^3D_2	0	3.1	4.8	6.1	0	0.5	0.7	1.2	16.4	83.6
1^3D_3	2.2	2.0	2.6	6.6	0.4	0.4	0.5	1.2	15.9	84.1

Table 5. Hadronic decay widths (in MeV) of the beauty-charm mesons.

State	BD	BD^*	B^*D	B^*D^*	$B_s D_s$	$B_s D_s^*$	$B_s^* D_s$	$B_s^* D_s^*$	Total
3^1S_0	0	0	109	0	0	0	0	0	109
3^3S_1	10	0	57	0	0	0	0	0	67
2^3P_2	3	0	0	0	0	0	0	0	3
2^3D_1	2	28	1	22	7	0	0	0	60
$2D$	0	15	4	37	0	0	0	0	57
$2D'$	0	64	69	68	0	0	0	0	201
2^3D_3	27	4	30	15	0	0	0	0	76

mainly decay into BD^* and B^*D^* with predicted widths of 15 and 37 MeV. Furthermore, the $B_c(2D')$ can mainly decay into BD^* , B^*D , and B^*D^* with predicted widths of 64, 69, and 68 MeV. The mixing angle of the two states is -43.9° . Furthermore, $B_c(2^3D_3)$ have three major decay channels of BD , B^*D , and B^*D^* with a decay width of 27, 30 and 15 MeV, respectively. These differences in decays will aid in distinguishing these excited beauty-charm meson states.

IV. SUMMARY

We calculated the mass spectrum and two-body hadronic decays for beauty-charm mesons based on the coupled channel framework. The coupled channel effects are calculated from 3P_0 model. The wave functions in our calculations are obtained by solving the Hamiltonian of the potential model with Gaussian Expansion Method.

Our results indicate that all beauty-charm states have coupled channel components, with each state having a

different composition. In general, the coupled channel effects are smaller for bound states compared to excited states. Furthermore, $1S$ states are approximately 3% – 5%, while the $1P$ states are approximately 8% – 11%. The $1D$ states are approximately 15% – 18%, and the $2S$ states are approximately 14% – 15%. Four $2P$ states have larger couple channel components of approximately 32% – 34%. The mixing angles of $1P$, $2P$, $1D$, and $2D$ states are determined as -35.0° , -36.3° , -42.8° and -43.9° , respectively.

For the strong decays of excited states above BD threshold, the $B_c(3^1S_0)$ state mainly strongly decays to B^*D channel and the $B_c(3^3S_1)$ mainly strongly decays to BD and B^*D . Furthermore, the $B_c(2^3P_2)$ mainly decays to BD . Additionally, $B_c(3S)$ and $B_c^*(3S)$ can be also detected in $B_c(3S) \rightarrow B_c(1S/2S) + \pi^+ + \pi^-$ and $B_c^*(3S) \rightarrow B_c(1S/2S) + \pi^+ + \pi^- + \gamma$ processes practically. For four D -wave states, the $B_c(2D')$ dominantly decays to BD^* , B^*D , and B^*D^* final states with a total width of 201 MeV. However, $B_c(2^3D_1)$, $B_c(2D)$, and $B_c(2^3D_3)$ states have

smaller decay widths of approximately 57–76 MeV. For the electromagnetic and weak decays of beauty-charm mesons, including polarization analysis, one can refer to Refs. [72–77].

Only a few beauty-charm meson states have been ob-

served in current experiments. Theoretical studies will be valuable in uncovering their nature and advancing experimental discoveries at the LHC and the future Tera-Z factory at CEPC.

References

- [1] R. L. Workman *et al.* (Particle Data Group), *PTEP* **2022**, 083C01 (2022)
- [2] F. Abe *et al.* (CDF), *Phys. Rev. Lett.* **81**, 2432 (1998), arXiv: hep-ex/9805034
- [3] G. Aad *et al.* (ATLAS), *Phys. Rev. Lett.* **113**, 212004 (2014), arXiv: 1407.1032
- [4] A. M. Sirunyan *et al.* (CMS), *Phys. Rev. Lett.* **122**, 132001 (2019), arXiv: 1902.00571
- [5] R. Aaij *et al.* (LHCb), *Phys. Rev. Lett.* **122**, 232001 (2019), arXiv: 1904.00081
- [6] N. Akbar, *Phys. Atom. Nucl.* **83**, 634 (2020), arXiv: 1911.02078
- [7] Q. Li, M.-S. Liu, L.-S. Lu *et al.*, *Phys. Rev. D* **99**, 096020 (2019), arXiv: 1903.11927
- [8] I. Asghar, F. Akram, B. Masud *et al.*, *Phys. Rev. D* **100**, 096002 (2019), arXiv: 1910.02680
- [9] N. Akbar, F. Akram, B. Masud *et al.*, *Eur. Phys. J. A* **55**, 82 (2019), arXiv: 1811.07552
- [10] A. P. Monteiro, M. Bhat, and K. B. Vijaya Kumar, *Phys. Rev. D* **95**, 054016 (2017), arXiv: 1608.05782
- [11] T.-Y. Li, L. Tang, Z.-y. Fang *et al.*, *Phys. Rev. D* **108**, 034019 (2023), arXiv: 2204.14258
- [12] X.-J. Li, Y.-S. Li, F.-L. Wang *et al.*, *Eur. Phys. J. C* **83**, 1080 (2023), arXiv: 2308.07206
- [13] Z.-B. Gao, Y.-Y. Fan, H. Chen *et al.*, (2024), arXiv: 2402.10629
- [14] S. Godfrey and N. Isgur, *Phys. Rev. D* **32**, 189 (1985)
- [15] L. Chang, M. Chen, X.-Q. Li *et al.*, *Few Body Syst.* **62**, 4 (2021), arXiv: 1912.08339
- [16] C. A. Dominguez, K. Schilcher, and Y. L. Wu, *Phys. Lett. B* **298**, 190 (1993)
- [17] S. S. Gershtein, V. V. Kiselev, A. K. Likhoded *et al.*, *Phys. Rev. D* **51**, 3613 (1995), arXiv: hep-ph/9406339
- [18] E. Bagan, H. G. Dosch, P. Gosdzinsky *et al.*, *Z. Phys. C* **64**, 57 (1994), arXiv: hep-ph/9403208
- [19] W. Chen, T. G. Steele, and S.-L. Zhu, *J. Phys. G* **41**, 025003 (2014), arXiv: 1306.3486
- [20] Z.-G. Wang, *Eur. Phys. J. A* **49**, 131 (2013), arXiv: 1203.6252
- [21] J. Zeng, J. W. Van Orden, and W. Roberts, *Phys. Rev. D* **52**, 5229 (1995), arXiv: hep-ph/9412269
- [22] L. Chang, M. Chen, and Y.-X. Liu, *Phys. Rev. D* **102**, 074010 (2020), arXiv: 1904.00399
- [23] M. Chen, L. Chang, and Y.-X. Liu, *Phys. Rev. D* **101**, 056002 (2020), arXiv: 2001.00161
- [24] C. T. H. Davies, K. Hornbostel, G. P. Lepage *et al.*, *Phys. Lett. B* **382**, 131 (1996), arXiv: hep-lat/9602020
- [25] G. M. de Divitiis, M. Guagnelli, R. Petronzio *et al.*, *Nucl. Phys. B* **675**, 309 (2003), arXiv: hep-lat/0305018
- [26] I. F. Allison, C. T. H. Davies, A. Gray *et al.* (HPQCD, FNAL Lattice, UKQCD), *Nucl. Phys. B Proc. Suppl.* **140**, 440 (2005), arXiv: hep-lat/0409090
- [27] Y. Lu, M. N. Anwar, and B.-S. Zou, *Phys. Rev. D* **94**, 034021 (2016), arXiv: 1606.06927
- [28] J.-F. Liu and G.-J. Ding, *Eur. Phys. J. C* **72**, 1981 (2012), arXiv: 1105.0855
- [29] J. Ferretti, G. Galata, E. Santopinto *et al.*, *Phys. Rev. C* **86**, 015204 (2012)
- [30] Y. S. Kalashnikova, *Phys. Rev. D* **72**, 034010 (2005), arXiv: hep-ph/0506270
- [31] B.-Q. Li, C. Meng, and K.-T. Chao, *Phys. Rev. D* **80**, 014012 (2009), arXiv: 0904.4068
- [32] J. Ferretti, G. Galat'a, and E. Santopinto, *Phys. Rev. C* **88**, 015207 (2013), arXiv: 1302.6857
- [33] Q. Deng, R.-H. Ni, Q. Li *et al.*, (2023), arXiv: 2312.10296
- [34] J. Ferretti and E. Santopinto, *Phys. Rev. D* **90**, 094022 (2014), arXiv: 1306.2874
- [35] E. van Beveren and G. Rupp, *Eur. Phys. J. C* **32**, 493 (2004), arXiv: hep-ph/0306051
- [36] E. van Beveren and G. Rupp, *Phys. Rev. Lett.* **91**, 012003 (2003), arXiv: hep-ph/0305035
- [37] S. Coito, G. Rupp, and E. van Beveren, *Phys. Rev. D* **84**, 094020 (2011), arXiv: 1106.2760
- [38] D. S. Hwang and D.-W. Kim, *Phys. Lett. B* **601**, 137 (2004), arXiv: hep-ph/0408154
- [39] Y. A. Simonov and J. A. Tjon, *Phys. Rev. D* **70**, 114013 (2004), arXiv: hep-ph/0409361
- [40] I. W. Lee, T. Lee, D. P. Min *et al.*, *Eur. Phys. J. C* **49**, 737 (2007), arXiv: hep-ph/0412210
- [41] F.-K. Guo, S. Krewald, and U.-G. Meissner, *Phys. Lett. B* **665**, 157 (2008), arXiv: 0712.2953
- [42] Z.-Y. Zhou and Z. Xiao, *Phys. Rev. D* **84**, 034023 (2011), arXiv: 1105.6025
- [43] A. M. Badalian, Y. A. Simonov, and M. A. Trusov, *Phys. Rev. D* **77**, 074017 (2008), arXiv: 0712.3943
- [44] Y.-B. Dai, X.-Q. Li, S.-L. Zhu *et al.*, *Eur. Phys. J. C* **55**, 249 (2008), arXiv: hep-ph/0610327
- [45] W. Hao, Y. Lu, and B.-S. Zou, *Phys. Rev. D* **106**, 074014 (2022), arXiv: 2208.10915
- [46] J.-J. Yang, W. Hao, X. Wang *et al.*, *Eur. Phys. J. C* **83**, 1098 (2023), arXiv: 2303.11815
- [47] O. Lakhina and E. S. Swanson, *Phys. Lett. B* **650**, 159 (2007), arXiv: hep-ph/0608011
- [48] Q.-F. Lü, T.-T. Pan, Y.-Y. Wang *et al.*, *Phys. Rev. D* **94**, 074012 (2016), arXiv: 1607.02812
- [49] D.-M. Li, P.-F. Ji, and B. Ma, *Eur. Phys. J. C* **71**, 1582 (2011), arXiv: 1011.1548
- [50] W. Hao, Y. Lu, and E. Wang, *Eur. Phys. J. C* **83**, 520 (2023), arXiv: 2212.10068
- [51] X.-C. Feng, W. Hao, and I.-J. Liu, *Int. J. Mod. Phys. E* **31**, 2250066 (2022), arXiv: 2205.07169
- [52] W. Hao, G.-Y. Wang, E. Wang *et al.*, *Eur. Phys. J. C* **80**, 626 (2020), arXiv: 1909.13099
- [53] S. Godfrey and R. Kokoski, *Phys. Rev. D* **43**, 1679 (1991)
- [54] E. Hiyama, Y. Kino, and M. Kamimura, *Prog. Part. Nucl. Phys.* **51**, 223 (2003)

- [55] H. Wang, Z. Yan, and J. Ping, *Eur. Phys. J. C* **75**, 196 (2015), arXiv: [1412.7068](#)
- [56] H. Wang, Y. Yang, and J. Ping, *Eur. Phys. J. A* **50**, 76 (2014)
- [57] E. P. Inyang, E. P. Inyang, E. S. William *et al.*, (2020), arXiv: [2012.10639](#)
- [58] E. M. Khokha, M. Abu-Shady, and T. A. Abdel-Karim, (2016), arXiv: [1612.08206](#)
- [59] M. Abu-Shady, T. A. Abdel-Karim, and S. Y. EzzAlarab, *J. Egyptian Math. Soc.* **27**, 14 (2019), arXiv: [1901.00470](#)
- [60] R. Rani, S. B. Bhardwaj, and F. Chand, *Commun. Theor. Phys.* **70**, 179 (2018)
- [61] S. Godfrey, *Phys. Rev. D* **70**, 054017 (2004), arXiv: [hepph/0406228](#)
- [62] D. Ebert, R. N. Faustov, and V. O. Galkin, *Phys. Rev. D* **67**, 014027 (2003), arXiv: [hep-ph/0210381](#)
- [63] N. Mathur, M. Padmanath, and S. Mondal, *Phys. Rev. Lett.* **121**, 202002 (2018), arXiv: [1806.04151](#)
- [64] L. Micu, *Nucl. Phys. B* **10**, 521 (1969)
- [65] A. Le Yaouanc, L. Oliver, O. Pene *et al.*, *Phys. Rev. D* **8**, 2223 (1973)
- [66] A. Le Yaouanc, L. Oliver, O. Pene *et al.*, *Phys. Rev. D* **9**, 1415 (1974)
- [67] P. Geiger and N. Isgur, *Phys. Rev. D* **44**, 799 (1991)
- [68] B. Silvestre-Brac and C. Gignoux, *Phys. Rev. D* **43**, 3699 (1991)
- [69] P. Geiger and N. Isgur, *Phys. Rev. Lett.* **67**, 1066 (1991)
- [70] P. Geiger and N. Isgur, *Phys. Rev. D* **55**, 299 (1997), arXiv: [hep-ph/9610445](#)
- [71] P. G. Ortega, J. Segovia, D. R. Entem *et al.*, *Eur. Phys. J. C* **80**, 223 (2020), arXiv: [2001.08093](#)
- [72] Y. Geng, M. Cao, and R. Zhu, (2023), arXiv: [2310.03425](#)
- [73] K. Chen, Y. Geng, Y. Jin *et al.*, (2024), arXiv: [2404.06221](#)
- [74] W. Tao, R. Zhu, and Z.-J. Xiao, *Phys. Rev. D* **106**, 114037 (2022), arXiv: [2209.15521](#)
- [75] W. Wang and R. Zhu, *Int. J. Mod. Phys. A* **34**, 1950195 (2019), arXiv: [1808.10830](#)
- [76] R. Zhu, *Nucl. Phys. B* **931**, 359 (2018), arXiv: [1710.07011](#)
- [77] C.-F. Qiao, P. Sun, D. Yang *et al.*, *Phys. Rev. D* **89**, 034008 (2014), arXiv: [1209.5859](#)